INCAST 2008-056

RANS COMPUTATIONS FOR FLOW THROUGH
A VARIABLE MACH NUMBER FLEXIBLE NOZZLE AT MACH 4

Vimala Dutta[1], P. K. Dutta[2] and Sharanappa V. Sajjan[3]
Computational and Theoretical Fluid Dynamics Division, N.A.L., Bangalore 560 017,
Council of Scientific and Industrial Research, India.
[1] vimala@ctfd.cmmacs.ernet.in, [2] pkd@ctfd.cmmacs.ernet.in, [3] svsajjan@ctfd.cmmacs.ernet.in

ABSTRACT: *Numerical simulation of flow through a Variable Mach number Flexible Nozzle (VMFN) at Mach 4 is carried out using the CFD code IMPRANS to validate the design of the nozzle based on the method of characteristics with boundary layer correction. The CFD analysis for the contour uses an implicit Reynolds-averaged Navier-Stokes (RANS) solver with Baldwin-Lomax turbulence model. Detailed flow characteristics like the centerline Mach number distribution and Mach contours of the steady flow through the converging – diverging nozzle are obtained to study and assess the suitability of the design.*

1. INTRODUCTION

The standard method for the design of a convergent – divergent nozzle to supply uniform flow with the design Mach number at the wind tunnel test section is based on the method of characteristics [19] with boundary layer correction. However, it is important to check the validity of the design by other means before taking up the fabrication of the nozzle, instead of waiting for the actual tunnel measurement. With the availability of advanced numerical techniques to solve the full Reynolds-averaged Navier-Stokes (RANS) equations, it is now possible to obtain detailed flow field inside the nozzle, which can provide valuable input to assess the suitability of the design.

The present work describes the application of an implicit Reynolds-averaged Navier-Stokes code (IMPRANS), developed at the CTFD division of National Aerospace Laboratories (NAL), Bangalore, to the Mach 4 contour of a Variable Mach number Flexible Nozzle (VMFN). The VMFN has been designed to augment the testing capability of the existing 0.6m × 0.6m transonic wind tunnel at the National Trisonic Aerodynamic Facility (NTAF) of NAL to supersonic range of Mach numbers upto 4. The RANS solver [4-10] is based on an implicit finite volume nodal point scheme wherein a control volume is formed by joining the centroids of the neighbouring cells around a nodal point in the computational domain. The numerical scheme for solving the two- and three-dimensional Reynolds-averaged Navier-Stokes equations governing steady and unsteady viscous compresssible flow has been derived indigenously by using Euler's implicit time differencing formula with nodal point spatial discretization. Certain basic ideas from the implicit finite difference scheme of Beam and Warming [2] and Steger [20], the nodal point schemes of Ni [16] and Hall [12], the Runge Kutta time-stepping scheme of Jameson et al. [15] and the cell-centered schemes due to Hollanders and Viviand [14] and Hollanders et al. [13] have been combined efficiently to evolve the present method. The code has been applied successfully for simulating compressible flow around stationary or moving bodies like aerofoils, wings, helicopter rotor and wind turbine blades [3-11,18]. The algebraic eddy viscosity model due to Baldwin and Lomax is used for turbulence closure [1].

2. NUMERICAL METHOD

The Reynolds-averaged Navier-Stokes equations that govern three-dimensional compressible viscous flows can be written in nondimensional conservative form as

$$\frac{\partial U}{\partial t} + \frac{\partial E}{\partial x} + \frac{\partial F}{\partial y} + \frac{\partial G}{\partial z} = 0 \qquad (1)$$

Here, U is the vector of conserved variables, E, F and G are flux vectors, (x,y,z) is the Cartesian coordinate system and t is the time variable.

Applying Euler's implicit time differencing formula

$$U^n = U^{n+1} - \left(\frac{\partial U}{\partial t}\right)^{n+1} \Delta t + O\left(\Delta t^2\right) \tag{2}$$

to equations (1), we obtain

$$\Delta U^n + \Delta t \left[\frac{\partial E}{\partial x} + \frac{\partial F}{\partial y} + \frac{\partial G}{\partial z}\right]^{n+1} = 0 \tag{3}$$

Here $U^n = U(t) = U(n\Delta t)$ is the solution vector at time level n and $\Delta U^n = \left(U^{n+1} - U^n\right)$ is the change in U^n over time step Δt. In order to facilitate the finite volume formulation, the above equations are written in the integral form as

$$\iiint_\Omega \Delta U^n dxdydz + \Delta t \iint_\Gamma \left[E^{n+1} e_x + F^{n+1} e_y + G^{n+1} e_z\right]. n\, dS = 0 \cdot \tag{4}$$

where Ω is any three-dimensional flow domain, Γ is the boundary surface and n is the unit vector normal to the surface bounding the control volume in the outward direction.

In the nodal point finite volume approach [4-10], the flow variables are associated with each mesh point (i, j, k) of the grid and the integral conservative equations are applied to each control volume Ω_{ijk} obtained by joining the centroids of the eight neighbouring hexahedron cells surrounding the nodal point. Application of nodal point spatial discretization to equations (4) leads to

$$\Delta U^n_{ijk} + \frac{\Delta t}{\Omega_{ijk}} \sum_{m=1}^{m=6} \left[(E_I - E_V)_m^{n+1} S_{mx} + (F_I - F_V)_m^{n+1} S_{my} + (G_I - G_V)_m^{n+1} S_{mz}\right] = 0, \tag{5}$$

where S_{mx}, S_{my} and S_{mz} are the x, y and z components of the surface vector corresponding to the m-th surface of the control volume. Linearizing the changes in flux vectors using Taylor's series expansions in time and assuming locally constant transport properties, equations (5) can be simplified to, after omitting superscript n,

$$\Delta U^n_{ijk} + \frac{\Delta t}{\Omega_{ijk}} \sum_{m=1}^{6} \left\{ \left[\left(A - \frac{\partial E_R}{\partial x}\right)\Delta U\right]_m S_{mx} + \left[\left(B - \frac{\partial F_S}{\partial y}\right)\Delta U\right]_m S_{my} + \left[\left(C - \frac{\partial G_T}{\partial z}\right)\Delta U\right]_m S_{mz} \right\}$$

$$= \frac{\Delta t}{\Omega_{ijk}} \sum_{m=1}^{6} \left[(E_I - E_V)_m S_{mx} + (F_I - F_V)_m S_{my} + (G_I - G_V)_m S_{mz}\right] \tag{6}$$

Here $A = \partial E_I / \partial U$, $B = \partial F_I / \partial U$, $C = \partial G_I / \partial U$, $E_R = \partial E_{V1}/ \partial U_x$, $F_S = \partial F_{V2}/ \partial U_y$ and $G_T = \partial G_{V3}/ \partial U_z$ are the Jacobian matrices, E_I, F_I and G_I are the inviscid flux vectors and E_V, F_V and G_V are the viscous flux vectors.

It may be noted here that the surface integrals in equations (4) are evaluated by summing up the contributions due to the flux terms over the six faces of the computational cell. The terms containing inviscid flux vectors are calculated by using the flow variables at the six neighbouring points and the derivatives in the viscous flux terms are discretized directly in the physical plane using Taylor's series expansions. The resulting block tridiagonal system of equations is solved by using a suitable block tridiagonal solution algorithm and proper initial and boundary conditions. A blend of second and fourth order artificial dissipation terms [17] is added explicitly to ensure convergence and to suppress oscillations near shock waves. Implicit second order dissipation terms are also added to improve the practical stability bound of the implicit scheme.

3. NUMERICAL SIMULATION OF FLOW THROUGH VMFN

For simulating flow through the Variable Mach number Flexible Nozzle, subsonic inflow conditions are imposed at the inlet while the static pressure corresponding to the exit Mach number is prescribed at the supersonic outlet. No-slip condition for velocity and adiabatic wall condition for temperature are applied at the walls of the converging – diverging nozzle. At the exit, all the variables except pressure are extrapolated from the interior.

Computations have been carried out using IMPRANS for both 2-D and 3-D steady flows inside the Mach 4 contour of VMFN at a Reynolds number of *Re=30 million* by employing a $281 \times 91 \times 91$ grid. Fig.1 depicts the results for the 3-D laminar and turbulent flows in terms of the centerline Mach number distribution and Mach fields on the central vertical, central horizontal and exit planes of the nozzle. Here, the centerline Mach number distribution is also compared with the corresponding 2-D result. It is found that the exit Mach number for the turbulent case is lower than that for the laminar case due to larger boundary layer thickness. This can be more clearly seen from the centerline Mach fields. In addition, the 3-D case always predicts a lower Mach number than the 2-D case due to larger boundary layer thickness in the presence of the side walls. For the 3-D laminar and turbulent cases, the centerline exit Mach number is found to be 3.98 and 3.80 respectively. The thick boundary layer for the turbulent case, as seen from the figure, not only reduces the exit Mach number, but also reduces the region of maximum Mach number in the exit plane. The mid-plane vertical distributions of flow variables at different axial stations are shown in Fig.2 for the turbulent flow case. As expected, the Mach number, temperature, density and axial velocity profiles display variations only near the upper and lower walls of the nozzle but remain flat for most part of the cross section. The available uniform flow area also decreases as one proceeds downstream due to growing boundary layers on the walls and turns out to be about 25% of the tunnel area at the test section.

ACKNOWLEDGEMENT

REFERENCES

[1] Baldwin BS and Lomax H. Thin Layer Approximation and Algebraic Model for Separated Turbulent Flows. AIAA Paper No. 78-257, 1978.

[2] Beam RM and Warming RF. An Implicit Factored Scheme for the Compressible Navier-Stokes Equations. *AIAA J.*, 1978, 16, 4, 393-402.

[3] Dutta PK, Dutta V and Sharanappa. RANS Computation of Flow past Wind Turbine Blades. *Proceedings, Seventh Asian Computational Fluid Dynamics Conference (ACFD7),* Bangalore, Paper 8.1, November 26 – 30, 2007.

[4] Dutta V. An Implicit Finite Volume Nodal Point Scheme for the Solution of Two-Dimensional Compressible Navier-Stokes Equations., NAL SP-9315, NAL, Bangalore, July 1993, 51-59.

[5] Dutta V. Implicit 2-D Navier-Stokes Solver for Compressible Viscous Flow around Aerofoils. *Proceedings, First Asian Computational Fluid Dynamics Conference*, January 16 – 19, 1995, 2, 683-690.

[6] Dutta V. Navier-Stokes Solutions for Unsteady Compressible Flows. *J. Aero. Soc. India*, 1999, 51, 4, 238-251.

[7] Dutta V. Unsteady Navier-Stokes Computation for Compressible Flows. *Workshop on Concepts and Applications of Computational Fluid Dynamics*, Amrita Inst. Tech. Sci., Coimbatore, May15 – 19, 2000, 72-92.

[8] Dutta V and Dutta PK. Computation of Unsteady Compressible Flows Past Aerofoils in Motion. *Proceedings, Third Asian Computational Fluid Dynamics Conference,* December 7-11, 1998, 354-359.

[9] Dutta V, Dutta PK and Sharanappa. An Implicit RANS Solver for Unsteady Compressibe Flow Computations. NAL SP 0301, NAL, Bangalore, March 5, 2003, 65-86.

[10] Dutta V, Gopinath R and Dutta PK. Navier-Stokes Computation of Unsteady Flow over Aerofoils at High Angle of Attack. *Proc. CFD97,* Univ. Victoria, Canada, May 25-27, 1997, 16-33–16-38.

[11] Dutta V, Sharanappa and Dutta PK. Navier-Stokes Computations for a Helicopter Rotor Blade in Hover. *Proc. 8th Annual CFD Symposium,* CFD Division of Aeronautical Society of India, Bangalore, August 11-13, 2005.

[12] Hall MG. Cell Vertex Multigrid Scheme for Solution of the Euler Equations. RAE-TM Aero. 2029. Also in *Proc. Conf. on Num. Methods for Fluid Dyn.*, 1985, 303-345.

[13] Hollanders H, Lerat A and Peyret R. Three-Dimensional Calculation of Transonic Viscous Flows by an Implicit Method. *AIAA J.*, 1985, 23, 11, 1670-1678.

[14] Hollanders H and Viviand H. ***The Numerical Treatment of Compressible High Reynolds Number Flows. Computational Fluid Dynamics***, Vol. 2, Kollmann, W. (Ed.), Hemisphere Publishing Corporation, 1980, 1-65.

[15] Jameson A, Schmidt W and Turkel E. Numerical Solution of Euler Equations by Finite Volume Methods Using Runge-Kutta Time Stepping Schemes. AIAA Paper No. 81-1259, 1981.

[16] Ni RH. A Multiple Grid Scheme for Solving the Euler Equations. *AIAA J.*, 1982, 20, 1565- 1571.

[17] Pulliam TH. Implicit Solution Methods in Computational Fluid Dynamics. *App. Num. Math., (trans. IMACS),* 1986, 2, 6, 441-474.
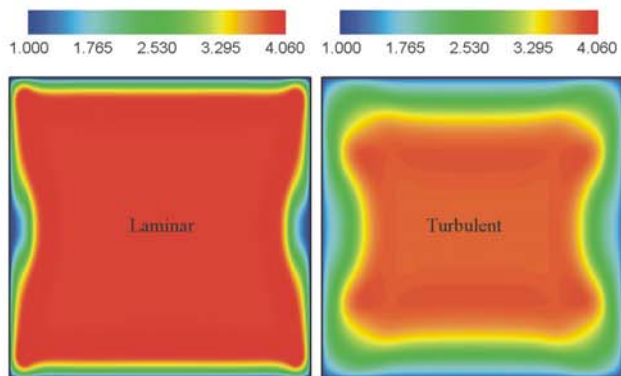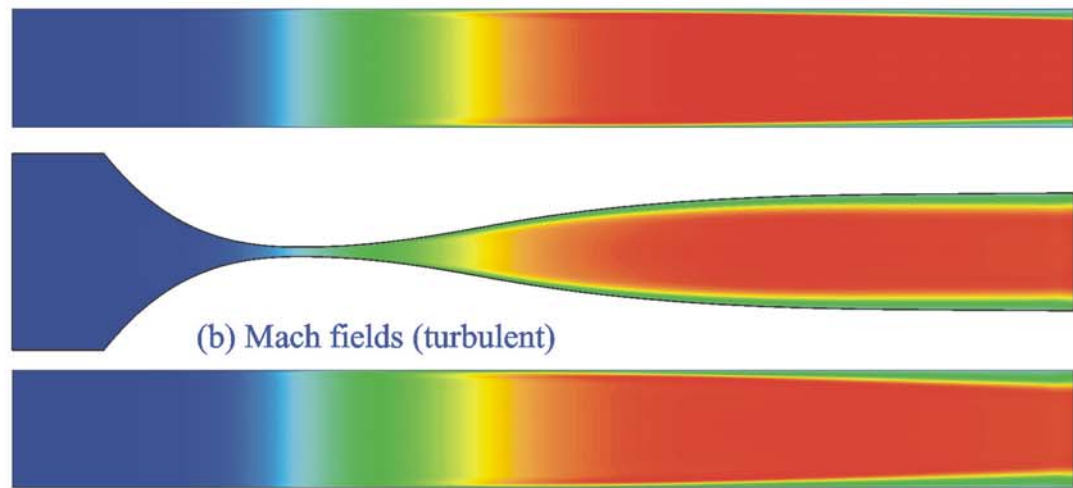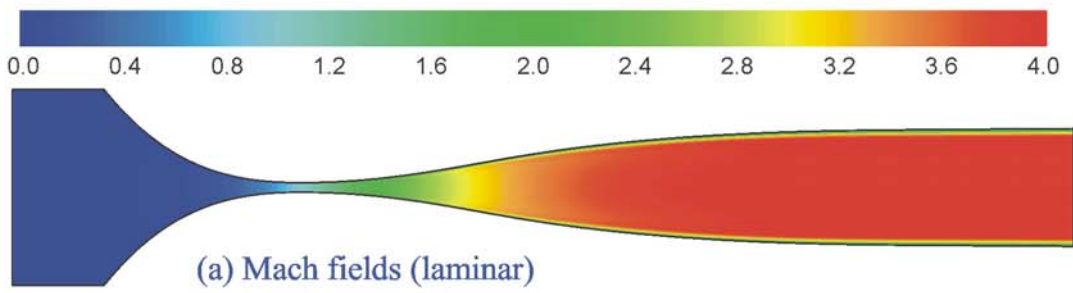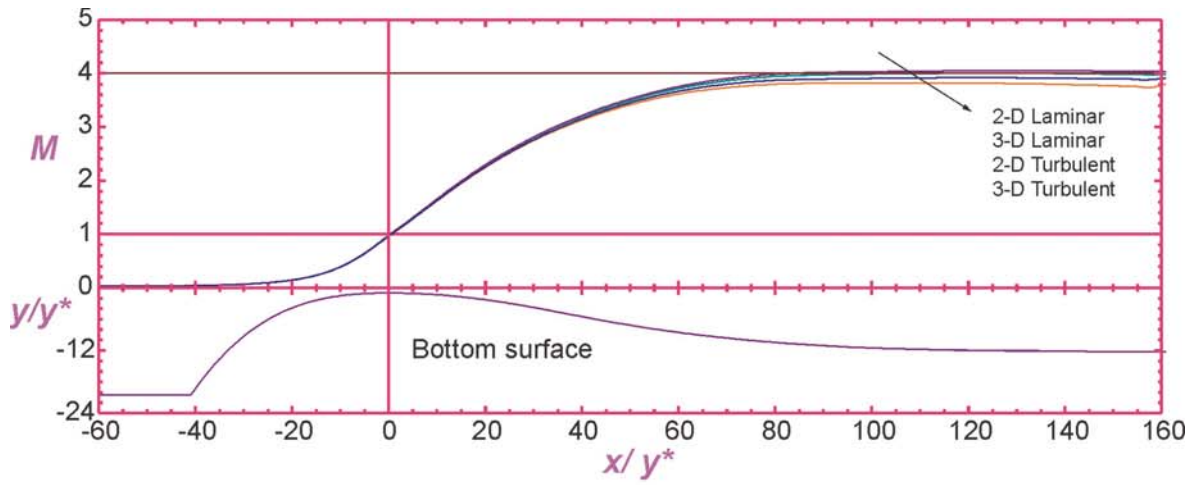
Fig. 1 Mach number distribution along the centerline and Mach fields on central vertical and horizontal planes and the exit plane of a Mach 4 nozzle for Re = 30 million

[18] Sharanappa, Dutta V and Dutta PK. Viscous Unsteady Flow around a Helicopter Rotor Blade in Forward Flight. *Proc. 9th Annual CFD Symposium,* CFD Division of Aeronautical Society of India, Bangalore, August 11-12, 2006.

[19] Sivells JC. Analytical Determination of Two-Dimensional Supersonic Nozzle Contours Having Continuous Curvature. AEDC-TR-56-11, July 1956.

[20] Steger JL. Implicit Finite Difference Simulation of Flow about Arbitrary Geometries with Application to Aerofoils. *AIAA J.*, 1978, 16, 679-686.
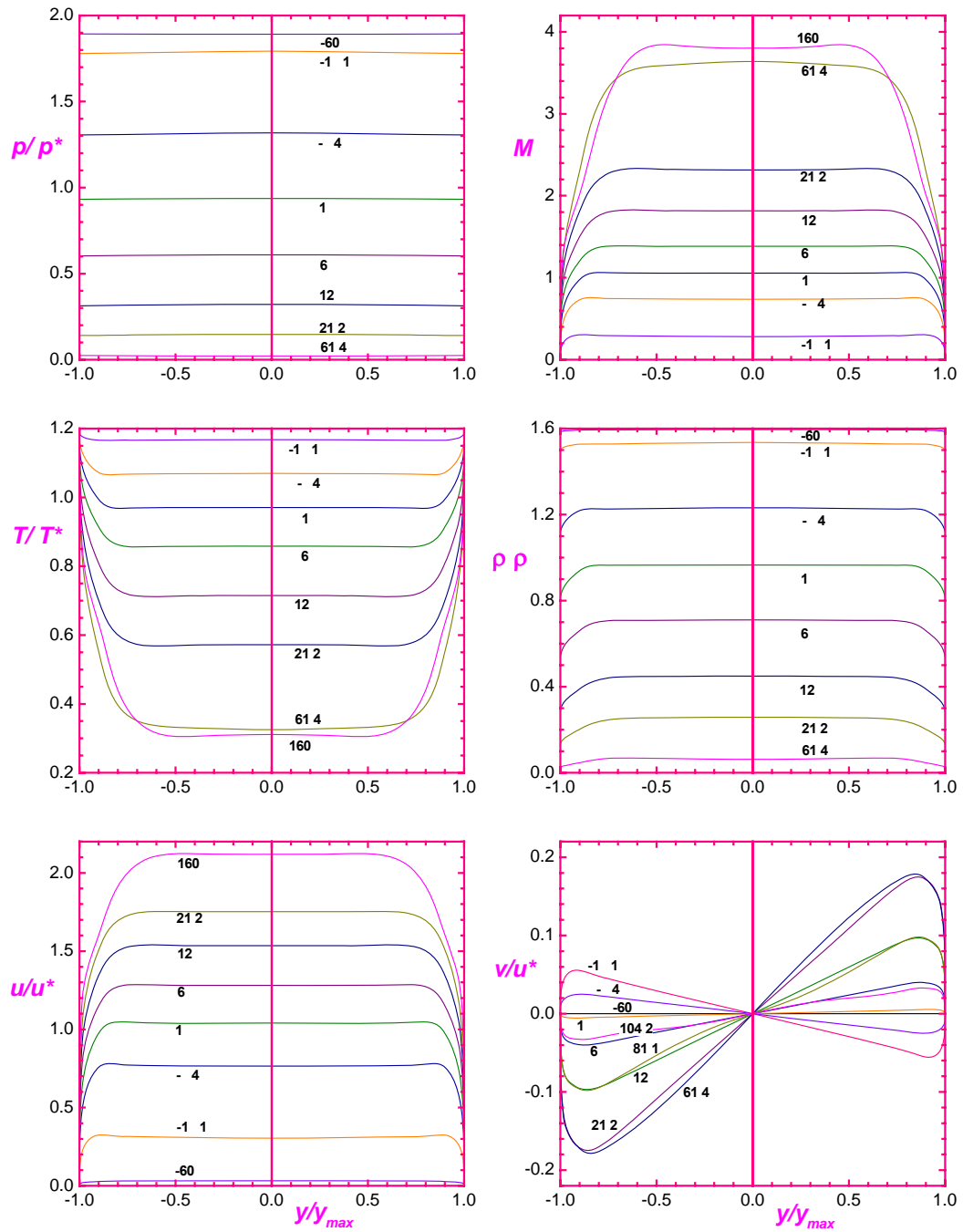
Fig. 2 Mid-plane vertical distributions of important flow characteristics at different axial locations for turbulent flow through Mach 4 nozzle at Re = 30 million